EFFECTS OF CONCAVE ROLLERS, CURVED-AXIS ROLLERS AND WEB CAMBER ON THE DEFORMATION AND TRANSLATION OF A MOVING WEB

by

J. L. Brown
Essex Systems
USA

ABSTRACT

A new method of analysis is applied to three problems that have resisted detailed solution. These are:

1. Concave roller
2. Curved-axis roller
3. Cambered web (Curvature of the relaxed web along its longitudinal axis)

In the first two of these, the primary interest is the stress/strain field near the downstream roller. In the third, the primary interest is the lateral translation. In all cases it is useful to have information on the stress field throughout the span to evaluate the potential for damage and wrinkling.

For each case, the normal strain and normal entry rules are used to develop downstream boundary conditions that can be used with a nonlinear version of the theory of elasticity for two-dimensional plane stress. A finite-element partial differential equation solver is used to develop steady-state solutions that include stress/strain fields and displacements throughout the spans.

Along with specific numerical examples, there is a discussion of implications for such things as wrinkling, spreading, lateral translation and overstressing.

A major advantage of the new method is that it provides a new way of looking at problems that will facilitate other approaches to modeling. This is illustrated by developing a beam theory model for cambered webs.

INTRODUCTION

The method of analysis for this work, called the P. D. E. model, is described in another paper [1] presented at this conference. It is based on a nonlinear form of two-dimensional elasticity theory and uses two boundary conditions for the downstream roller. One, called the normal strain rule is new. The other is an extended form of the normal entry rule. The purpose of this paper is to provide illustrative examples of how this new method can used to explore applications by analyzing the following:

1. Behavior of a concave roller
2. Behavior of a curved-axis roller
3. Behavior of a cambered web (Curvature of the relaxed web along its longitudinal axis)

In addition, insight gained from a P. D. E. model, is used to develop a beam model for cambered webs using methods similar to those of Shelton[2] in his work on the misaligned roller. The two models are compared and shown to be in excellent agreement.

The P. D. E. solver software for this work, running on an ordinary 2.8 GHz PC, produced solutions to problems in times ranging from 1 to 10 minutes.

NOMENCLATURE

A	Cross sectional area of web, m^2
D	Roller diameter, m
G	Shear modulus, Pa
h	Web thickness, m
I	Moment of inertia, m^4
L	Length of span, m
M	Moment, Nm
N	Force, N
Q_i	Mass flow rate per unit of relaxed area at upstream roller, Kg/s
Q_o	Mass flow rate per unit of relaxed area at downstream roller, Kg/s
R_w	Radius of camber of relaxed web, m
T	Tension, N
T_{avg}	Cross web average of tension, N
u	Particle displacement in x direction, m
u_y	Derivative of u with respect to y
v	Particle displacement in y direction, m
v_x	Derivative of v with respect to x
V_y	Velocity in the y direction, m/s
V_u	Surface velocity of upstream roller, m/s
V_d	Surface velocity of downstream roller, m/s
W	Width of web, m
y_c	y displacement relative to y = 0, m
y'	y displacement relative to curve of camber, m
γ_{xy}	Elastic shear strain
ε	Elastic strain
ε_o	Longitudinal strain at entry of upstream roller
η	Deformed y coordinate, m
θ_r	Angle of misaligned roller axis relative to y-axis (CCW positive), radians
θ_c	Angle of camber (inclination of downstream end relative to x-axis), radians

μ Poisson's ratio
ξ Deformed x coordinate, m
σ Stress, Pa
σ_n Stress normal to a boundary, Pa
τ_{xy} Shear stress in x,y plane, Pa
ψ Angle of tangent to particle trajectory of web (in relation to x-axis), radians
ω_z Elastic rotation in x,y plane

Subscripts

u Upstream
d Downstream
x Aligned with x-axis
y Aligned with y-axis
z Aligned with z-axis (normal to web plane)
b Displacement due only to bending
s Displacement due only to shear

ASSUMPTIONS

For this analysis, air film effects are ignored and it will be assumed that friction controls traction between the roller and web. The usual assumptions are made about the behavior of the web when it is on the roller. At the entry point, friction locks it onto the roller surface. Any strains existing at the point of entry are then frozen in place and remain fixed relative to the roller surface until the web reaches a zone at the exit where it begins to slip from the roller under the influence of stresses downstream. And the lines of contact at entrance and exit are assumed to be parallel to the roller axis. The turning torque of the roller is small in comparison to web tension and the "stick zone" will be a large percentage of the contact area. Under these conditions, the stresses in the upstream span are isolated from changes downstream.

Other assumptions: Viscoelastic and inertial effects are not significant. Thickness and material properties are constant in the longitudinal direction.

EARLIER WORK

Shelton [2] laid the groundwork for beam theory modeling of webs in his 1968 dissertation. Development of the cambered web model, presented here, follows his example.

Swanson [3] in his 1997 paper on web spreading devices provided a definitive demonstration of the spreading action of a concave roller by positioning a slitting blade immediately before the span he was observing. He used this to separate an inch of the web (0.8 mil PET) at the edge and measured the displacement of this piece at the downstream roller.

Swanson [4] in a later paper attempted to determine through experiment and analysis the boundary conditions and basic principles that could be used to extend beam models to include non-uniform webs. This work confirmed earlier observations that cambered webs deflect toward the slack edge (the convex side) and established bounds on values for an end moment that might account for the behavior.

Shelton [5] provided a good survey of the problems of cambered webs and provided qualitative insight by comparing their behavior to uniform webs on tapered rollers.

Markum and Good [6] confirmed Swanson's observations on the effect of a concave roller and developed a beam model that provided an estimate of the lateral displacement.

Olsen [7] proposed a beam model for non-uniform webs in which the camber was assumed to be induced by frozen-in strain.

PLANE STRESS DEFINITIONS

The following equations for plane stress are taken from Novoshilov's [8] simplified nonlinear theory for small rotations.

Displacements from the relaxed coordinates *x* and *y* are *u* and *v*, respectively. Strains are,

Strain in the x direction $\varepsilon_x = \dfrac{\partial u}{\partial x}$ (1)

Strain in the y direction $\varepsilon_y = \dfrac{\partial v}{\partial y}$ (2)

Shear strain $\gamma_{xy} = \dfrac{\partial v}{\partial x} + \dfrac{\partial u}{\partial y}$ (3)

$u_y = \dfrac{\partial u}{\partial y}$ (4) $v_x = \dfrac{\partial v}{\partial x}$ (5)

Strain in the *z* direction $\varepsilon_z = \dfrac{-\mu}{1-\mu}(\varepsilon_x + \varepsilon_y)$ (6)

Rotation in *x*,*y* plane $\omega_z = \dfrac{1}{2}\left(\dfrac{\partial v}{\partial x} - \dfrac{\partial u}{\partial y}\right)$. (7)

Deformed coordinates are,

$\xi = x + u$ (8) $\eta = y + v$ (9)

Assuming Hook's Law, the stresses may be expressed in terms of strains, Poisson's ratio, μ, and modulus of elasticity, *E*, as follows.

The x-axis stress is: $\sigma_x = \dfrac{E}{1-\mu^2}\left[\varepsilon_x + \mu\varepsilon_y\right]$ (10)

The y-axis stress is: $\sigma_y = \dfrac{E}{1-\mu^2}\left[\varepsilon_y + \mu\varepsilon_x\right]$ (11)

The shear stress is: $\tau_{xy} = \dfrac{E}{2(1+\mu)}\left[\dfrac{\partial u}{\partial y} + \dfrac{\partial v}{\partial x}\right]$ (12)

The equations of equilibrium are:

$$\frac{\partial}{\partial x}\left[\sigma_x - \omega_z\tau_{xy}\right] + \frac{\partial}{\partial y}\left[\tau_{xy} - \omega_z\sigma_y\right] = 0 \quad (13)$$

$$\frac{\partial}{\partial y}\left[\sigma_y + \omega_z\tau_{xy}\right] + \frac{\partial}{\partial x}\left[\tau_{xy} + \omega_z\sigma_x\right] = 0 \quad (14)$$

Another useful relationship is the expression that relates the *x* and *y* components of length of an infinitesimal line element before and after deformation.

$$d\xi = (1+\varepsilon_x)dx + u_y dy \qquad d\eta = v_x dx + (1+\varepsilon_y)dy \tag{15}$$

BOUNDARY CONDITIONS

Boundary conditions at a downstream roller will be based on the normal entry and normal strain rules [1],

$$\text{Normal Entry:} \quad \psi = \tan^{-1}\left[v_x dx + (1+\varepsilon_y)dy\right]\left[(1+\varepsilon_x)dx + u_y dy\right]^{-1} = \theta_r \tag{16}$$

where ψ is the angle of a vector tangent to a particle path in the web and

$$\text{Normal Strain}^1: \quad \varepsilon_x = 1 - \frac{V_u}{V_d}(1-\varepsilon_o) \ . \tag{17}$$

For a uniform web, (16) reduces to,

$$\tan^{-1} v_x (1+\varepsilon_x)^{-1} \approx v_x = \theta_r \ . \tag{18}$$

V_d and V_u are, respectively, the downstream and upstream roller surface velocities and it is understood that these may be a function of y. ε_o is the longitudinal strain at the entry to the upstream roller and may also be a function of (y + v) if the roller is nonuniform.

A COMPARISON OF A CONCAVE AND CURVED-AXIS SPREADER ROLLERS

A concave roller has a straight axis but a nonuniform diameter - smaller in the middle than at the edges. The depth profile is usually circular. The curved-axis roller has a uniform diameter. But, the axis is curved so that particle paths encounter a roller angle that increases with distance from the centerline.

The concave and curved-axis rollers could be named by the boundary condition that causes the spreading. In the case of the concave roller it would be called a normal strain spreader and in the case of the curved-axis roller it would be called a normal entry spreader.

A concave roller and a curved-axis roller will be compared in identical circumstances. The model parameters will be the same as one of the cases studied by Markum and Good [6] in their investigation of a concave roller. They evaluated spreading by splitting a web as it exited the upstream roller and measuring the separation at the spreader. The concave roller profile will be the same as Markum and Good's *Parabolic Roller 2*. The radius of curvature for the axis of the curved-axis roller will be chosen by trial-and-error to produce the same maximum spreading action as the concave roller. The test parameters are shown in Table 1. The maximum profile depth in one web width is 0.28 mm.

---

[1] This is based on approximation $(1+\varepsilon_x)^{-1} \approx (1-\varepsilon_x)$

Material	Modulus (Mpa)	Caliper (μm)	Width (m)	Length (m)	Tension (N)	Profile Radius (m)	Profile F(y)
LDPE	165.5	25.4	0.152	0.419	17.8	10.16	.02776 + .0492y^2

Table 1
Test parameters for Markum and Good experiment

Boundary Conditions for the Concave Roller

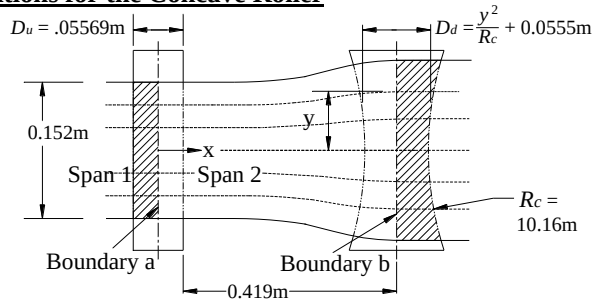

Figure 1
Concave roller

Two boundary conditions are needed for each of the four boundaries.

The sides are assumed to be unconstrained. So, for those boundaries the normal and tangential stresses will both be zero. Therefore,

$$\sigma_n = 0 \qquad \tau_n = 0 \ . \tag{19}$$

Boundary conditions at boundary "b" will be the normal entry and normal strain rules.

$$v_x = 0 \qquad (20) \qquad\qquad \varepsilon_x = 1 - \frac{V_u}{V_d}\left(1 - \varepsilon_o\right) \ . \tag{21}$$

Equation (21) may be put into a more convenient form if V_d is expressed as a fraction of V_u. And since a non-uniform roller will cause this ratio to vary with distance from the roller centerlines, V_d can be expressed as a function of the fractional difference in roller diameters. If *f(y)* is defined as,

$$f(y) = \frac{D_d(y) - D_u}{D_u} \tag{22}$$

where, D_d and D_u are the respective diameters of the downstream and upstream rollers and y is the distance from the roller centerlines. Then,

$$V_d = V_u \left[1 + f(y)\right] \qquad (23) \quad \text{and} \quad \varepsilon_x = 1 - \frac{V_u\left(1 - \varepsilon_o\right)}{V_u\left[1 + f(y)\right]} \cong \varepsilon_o + f(y) \ . \tag{24}$$

Note that the deformed y coordinate, $\eta = y + v$, may be used as the independent variable for *f(y)* where solution method allows it. This is done for the results reported here.

It will be assumed that span 1 is in pure tension with uniform, aligned rollers. So, the displacements at the entry to the upstream roller will determine the boundary conditions at "a". These are

$$v = -\mu\varepsilon_o y \qquad (25) \qquad\qquad u = 0\ . \qquad (26)$$

The roller profile in the Markum and Good experiment was a circular arc. The roller diameters and profile radius in Figure 1 have been chosen to match their values. Using these values equation (22) becomes,

$$f(y) = (1.767m^{-1})y^2 - .00340\,. \qquad (27)$$

Boundary Conditions for the Curved-axis Roller

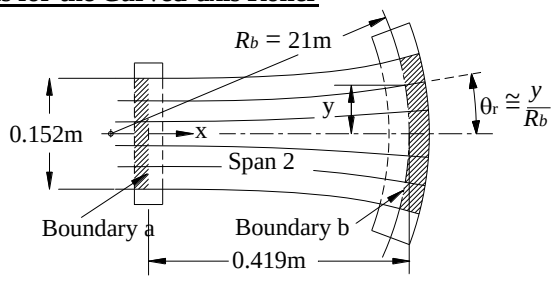

Figure 2
Curved-axis roller

Two boundary conditions will again be needed for each of the four boundaries.

The sides are assumed to be unconstrained. So, for those boundaries the normal and tangential stresses will both be zero. Therefore,

$$\sigma_n = 0 \qquad\qquad \tau_n = 0 \qquad (28)$$

where σ_n is the stress normal to the boundary and τ_n is the shear stress tangent to the boundary.

Boundary conditions at "b" will be the normal entry and normal strain rules,

$$v_x = \theta_r = \sin^{-1}\left(\frac{y}{R_b}\right) \cong \frac{y}{R_b} \qquad (29) \qquad\qquad \varepsilon_x = 1 - \frac{V_u}{V_d}\left(1-\varepsilon_o\right)\ . \qquad (30)$$

It will be assumed that span 1 is in pure tension with uniform, aligned rollers. So, the displacements at the entry to the upstream roller will determine the boundary conditions at "a". These are

$$v = -\mu y\varepsilon_o \qquad (31) \qquad\qquad u = 0\ . \qquad (32)$$

Results

One way to look at the spreading action of these rollers is to subtract out the Poisson contraction due to longitudinal stress. This can be done by using the constitutive equation (11). The net spreading strain, ε_s is due solely the cross web stress σ_y. Therefore,

$$\sigma_y \frac{1-\mu^2}{E} = \varepsilon_s = \varepsilon_y + \mu\varepsilon_x \qquad (33)$$

Figure 3 shows very little difference in the way the two rollers distribute the spreading. In both cases it drops off in a parabolic fashion from a peak in the middle to zero at the edges.

The *y* displacements are compared in Figure 4. The contours are not particle paths. But, they have similar slopes. The cross web stresses are shown in Figure 5. The curved-axis roller shows compressive stress. However, the levels are not high. There is also an area of compressive stress for the concave roller that is just beyond the area shown in the graph. It has a pattern similar to that of the curved-axis roller with an extreme of only –825 Pa.

The curved-axis roller had a radius of 21m. The concave roller had a profile radius of 10.16m and a minimum diameter of 55.5mm.

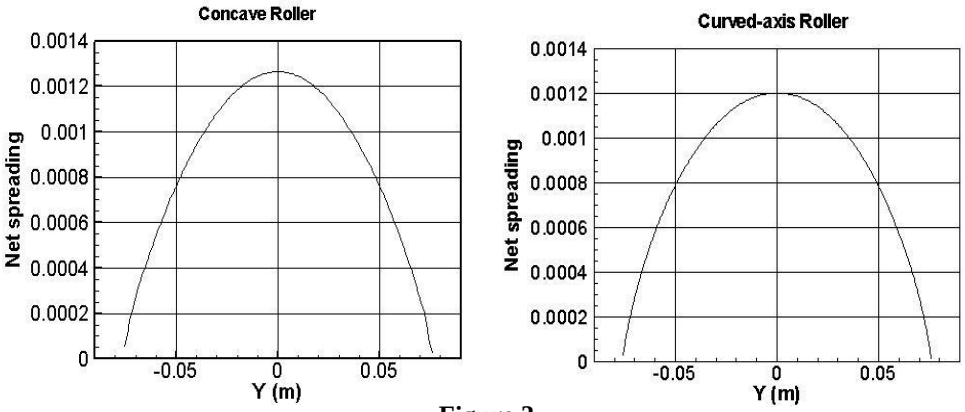

Figure 3

Comparison of spreading by Concave and Curved-Axis rollers

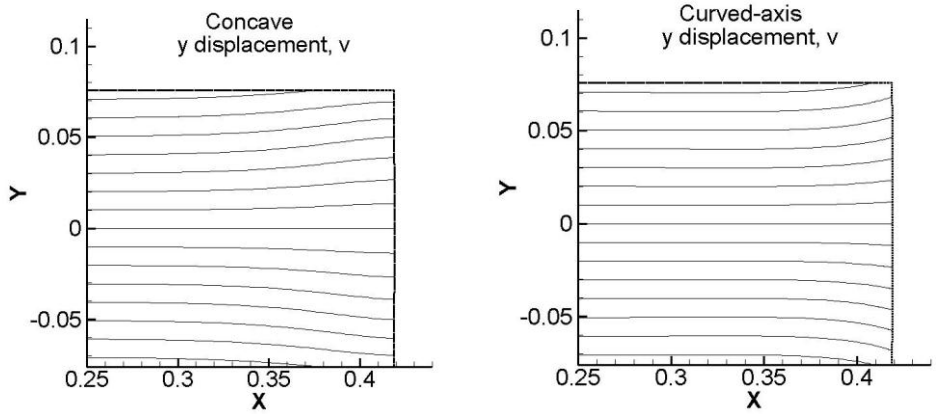

Figure 4

Comparison of *y* displacement, *v*, for concave and curved-axis rollers

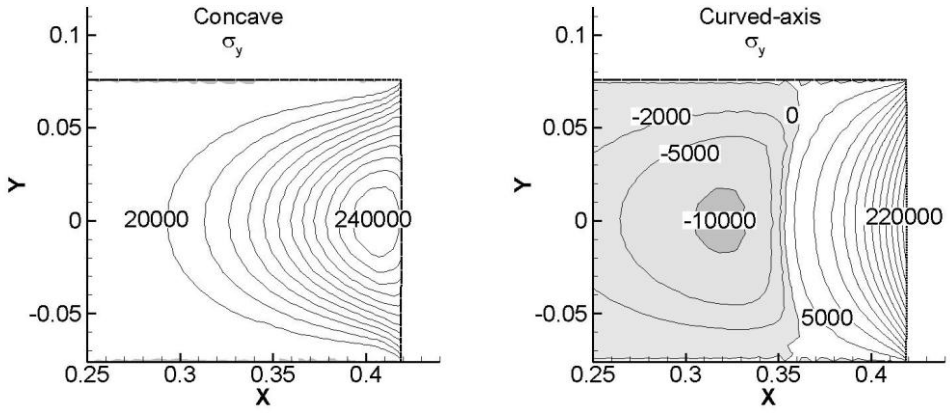

Figure 5
Comparison of cross web stress (Pa) for concave and curved-axis rollers

Magnification of Lateral Errors

There has been a presumption that because of the lateral shifts seen with tapered rollers, concave rollers would destabilize lateral registration. This was investigated by repeating the model calculations with a shift in the centerline of the profile. The result was that the centerline of the web moved opposite to the direction of profile shift. The shift was approximately – 11.6% of the profile shift. This relationship held for shifts up to ½ web width. Another way to think of it is that if the web shifted laterally by 1 inch at the upstream roller, it would shift in the same direction by 1.116 inch at the concave roller. When the roller profile radius was doubled, the ratio decreased to –5.5%. So, while it is true that the spreader magnifies any change in the upstream lateral position, the effect can be quite small if the spreading is kept modest.

There has never been any reason to suspect curved-axis rollers of destabilizing lateral registration. But, for the sake of curiosity this was investigated with the P. D. E. model by rerunning the parameters of the curved-axis roller with a shift in the centerline of the profile. The result was that, just as in the case of the concave roller, the centerline of the web moved opposite to the direction of profile shift. The shift, however, was significantly less. It was approximately –1.5% of the profile shift as opposed to –11.6% for a concave roller with the same spreading ability. This relationship also held for shifts up to ½ web width.

When the maintenance problems of curved-axis rollers are considered, a concave roller might often be a better choice.

APPLICATION TO A CAMBERED WEB

The analysis begins by assuming that a cambered web is created on a tapered core in the manner described by Swanson [3]. The roll is assumed to be formed in such a manner that the relaxed web will pay off from the roll with its edges normal to the roll axis.

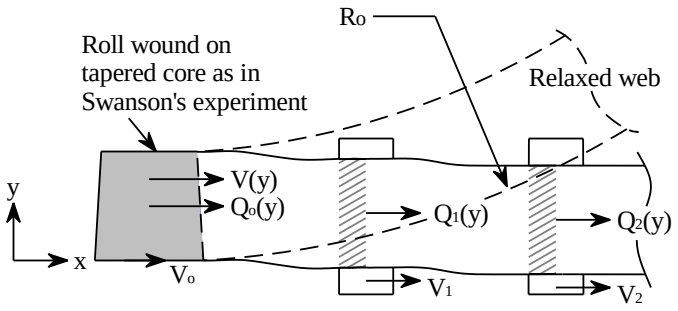

Figure 6
Normal Strain in a Cambered Web

Normal Strain Boundary Condition

The mass flow of the web at the line of exit from the unwinding roll will be,

$$Q_o = V_o\,(dy)\,\rho_o h\frac{R_o - y}{R_o} \tag{34}$$

where R_o is the radius of the outer edge, V_o is the surface velocity at the outer edge and y is the distance from the outer edge.

The mass flow at the entry to the first roller will be,

$$Q_1 = dy\left(1+\varepsilon_{y1}\right)\rho_1 h\left(1+\varepsilon_{z1}\right)V_1 \tag{35}$$

where ε_{y1} and ε_{z1} are the y and z strains at the entry to the first roller, ρ_1 is the density at the first roller, V_1 the circumferential velocity of the roller and h the web thickness. And using the mass density relationship,

$$\rho_1 = \frac{\rho_o}{\left(1+\varepsilon_{x1}\right)\left(1+\varepsilon_{y1}\right)\left(1+\varepsilon_{z1}\right)} \tag{36}$$

Q_1 becomes,

$$Q_1 = dy\,\rho_o h V_1\left(1+\varepsilon_{x1}\right)^{-1} \tag{37}$$

Equating Q_1 and Q_o and solving for ε_{x1} , the longitudinal strain at the entry to the first roller,

$$\varepsilon_{x1} = \frac{R_o}{R_o - y}\frac{V_1}{V_o} - 1 \tag{38}$$

At $y = 0$, equation (38) may be solved for the strain at the outer edge of the web at the entry to the first roller. This will be called ε_{xo} ,

$$\varepsilon_{xo} = \frac{V_1}{V_o} - 1\ . \qquad \text{So,} \qquad \frac{V_1}{V_o} = 1+\varepsilon_{xo}\ . \tag{39}$$

Substituting (39) into (38) yields,

$$\varepsilon_{x1} = \frac{R_o}{R_o - y}\left(1+\varepsilon_{xo}\right) - 1 \tag{40}$$

Using the same procedure for the second roller, the mass flow is,

$$Q_2 = dy\,\rho_o h V_2 \left(1+\varepsilon_{x2}\right)^{-1} \ . \tag{41}$$

Equating Q_1 and Q_2 and solving for ε_{x2} , the longitudinal strain at the entry to the second roller,

$$\varepsilon_{x2} = \frac{V_2}{V_1}\left(1+\varepsilon_{x1}\right)-1 \tag{42}$$

And finally, if the value for ε_{x1} in equation (38) is substituted in (42),

$$\varepsilon_{x2} = \frac{V_2}{V_1}\frac{R_o}{R_o - y}\left(1+\varepsilon_{xo}\right)-1 \tag{43}$$

So, in general, the expression for longitudinal strain at a downstream roller will be,

$$\varepsilon_x = \frac{V_d}{V_u}\frac{R_o}{R_o - y}\left(1+\varepsilon_{xo}\right)-1 \tag{44}$$

Where V_u and V_d are the upstream and downstream roller surface velocities and ε_{xo} is the value of longitudinal strain at the outer edge of the previous span. Looking back at the expression for ε_{x1} in (38), it is now evident that the strain relationship at the first roller following the unwinding roll is like the others except that ε_{xo} is zero.

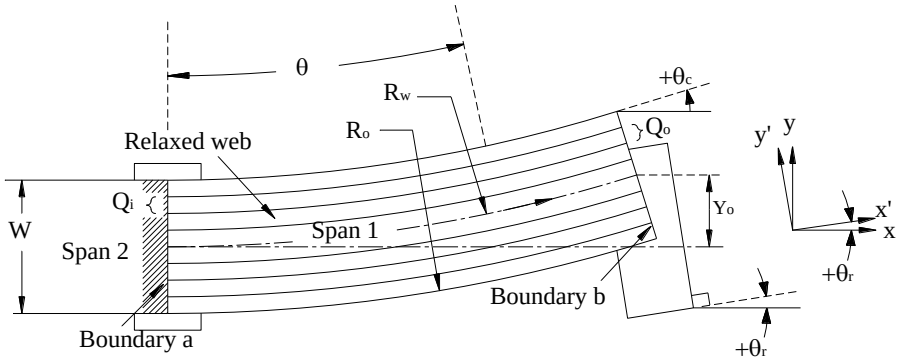

Figure 7
Parameters of Cambered Web for Development of Normal Entry Condition

Normal Entry Boundary Condition

With the P. D. E. method, all of the strains and displacements are defined in relation to the curved relaxed web. So, the normal entry rule will change to accommodate the fact that the particle trajectories of the relaxed cambered web are circular arcs. Starting with the defining equation for a the normal entry angle, equation (16), and since the relaxed trajectories are circular arcs of radius, *r*,

$$dy = -x/\left(r^2 - x^2\right)^{1/2}\, dx = \tan\theta\, dx \ . \tag{45}$$

At boundary "b", $\theta = \theta_c$ and the tangent of the normal entry angle is,

$$\psi = \tan^{-1}\left\{\left[v_x + \left(1+\varepsilon_y\right)\tan\theta_c\right]\left[\left(1+\varepsilon_x\right) + u_y \tan\theta_c\right]^{-1}\right\} = \theta_r \tag{46}$$

And equation (46) becomes,

$$\tan\theta_r\left[\left(1+\varepsilon_x\right) + u_y \tan\theta_c\right] = \left[v_x + \left(1+\varepsilon_y\right)\tan\theta_c\right] \tag{47}$$

Solving for v_x,

$$v_x = \tan\theta_r \left[\left(1+\varepsilon_x\right) + u_y \tan\theta_c \right] - \left(1+\varepsilon_y\right)\tan\theta_c \cong \theta_r - \theta_c \qquad (48)$$

where θ_c is the angle of camber and θ_r is the angle of the downstream roller.

Boundary conditions for the two edges are the same as in the other problems except that the outward normal and tangential components of stress are not aligned with the *x* or *y* axes. So, for rectangular coordinates the conditions are as follows.

$$\sigma_n = 0 = \sigma_x \cos^2\alpha + \sigma_y \sin^2\alpha + 2\tau_{xy}\sin\alpha\cos\alpha \qquad (49)$$

$$T_n = 0 = \left(\sigma_y - \sigma_x\right)\sin\alpha\cos\alpha + \tau_{xy}\left(\cos^2\alpha - \sin^2\alpha\right) \qquad (50)$$

σ_n is the normal component of stress, T_n is the tangential shear and α is the angle of the boundary-normal in relation to the *x*-axis.

Upstream Boundary Conditions

At the upstream roller, the *u* displacement will be,

$$u = 0\,. \qquad (51)$$

If span 2 has been analyzed, the results for its downstream roller can be used for *v*. In many cases, it will be sufficient to estimate it as follows. The ratio of σ_y to σ_x at the exit of span 2 is usually much less than μ, which means that the *v* can be approximated as a function of the strain, ε'_x at the exit of span 2. Furthermore, if the upstream roller is uniform, ε'_x will be an expression similar to (43).

$$v = -\mu\int \varepsilon'_x\, dy + C \quad . \qquad (52)$$

Since the only boundary conditions that control absolute position of the web are at boundary "a", the constant of integration, *C*, may be chosen arbitrarily to position the web at a convenient location.

Comparison with Swanson's [3] Results

An example is illustrated in Figure 8 . This is for one of the web geometries tested by Swanson: L = 2m, W = 0.3048m, E = 4.14e9Pa, Thickness = 23.4μm, Average longitudinal tension, T_{avg} = 32.5N (T_{avg} is larger than Swanson's value of 22N because the model indicates this is the value needed to avoid a slack edge), R_w = 139m. The P. D. E. model shows that when running, the web will move toward the convex side until it is almost straight with an offset from y = 0 of –18.1 microns. All stresses are in Pascals.

In general the P. D. E. model shows that

When running between parallel rollers cambered webs become almost straight.

The curvature at the downstream end becomes a small positive fraction of the relaxed value.

The longitudinal tension profile will increase linearly from a low value on the convex side to a maximum on the concave side.

For parallel rollers the cross web tension profile will be very uniform throughout the length of the span.

There will be some compressive cross web stress near the downstream roller that worsens with roller misalignment.

Some of the graphic data is shown in Figure 8. The offset of –18.1 microns does not agree precisely with Swanson's experimental results. He measured - 0.3 mm. However, it should be observed that 0.3 mm is only 2.0% of the initial displacement due to camber, Y_o = 14.4mm. So, his experiment correctly showed that the web became nearly straight. And this was evident in all of the nine experiments tabled in the paper. Furthermore, he correctly predicted that the curvature at the downstream roller would be between 0 and 1/*Rw*.

(a)

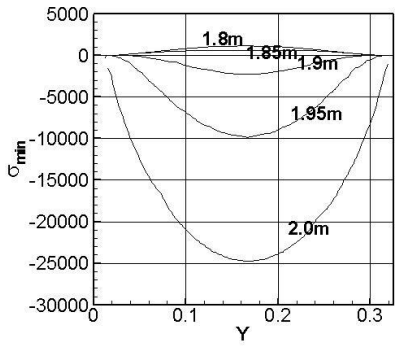

(b)

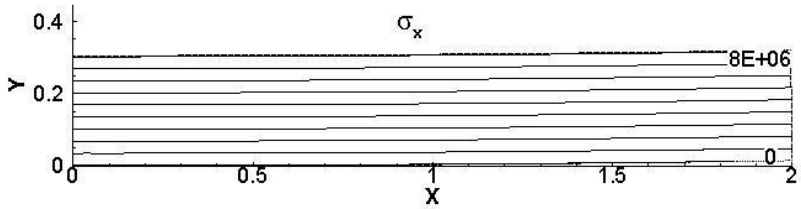

(c)

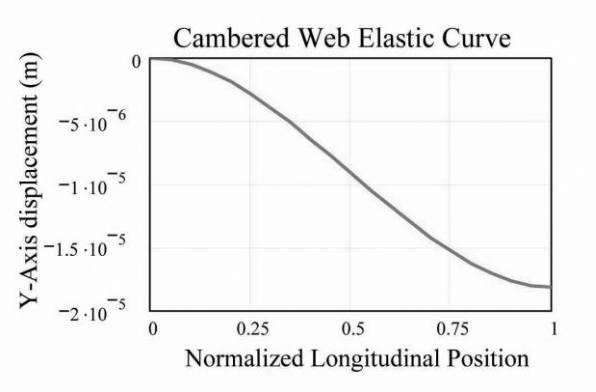

Figure 8
Results for Cambered Web
(a) Minimum principal stress near downstream roller (b) Contours of longitudinal stress (c) Elastic curve (neutral axis relative to y = 0)

There may also have been problems in the Swanson test due to the fact that the conditions upstream of the test span were not controlled well and/or because of the

difficulty of measuring such a small displacement on a moving web. There were actually two spans involved in the test. One was a very short run from the unwinding roll to the upstream roller of the main test span. Both of these were mounted on a four-bar linkage so that the side force could be measured. Although the tension in the main test span was carefully controlled, the tension between the unwind roll and the upstream roller was set by a friction brake with a manual adjustment. Therefore, the upstream conditions going into the test span are unknown. And as the foregoing analysis shows, this information is critical to predicting behavior of the test span.

BEAM MODEL FOR A CAMBERED WEB

A beam model is a useful adjunct to a P. D. E. numerical model. It can provide answers to many questions that are often adequate for applications. And it provides a conceptual framework for utilizing the P. D. E. results. So, one of the first things done with the P. D. E. model was to look for the *fourth boundary condition* necessary for a beam model solution. An obvious possibility is to use (43) to estimate the end moment. So long as $\sigma_y << \sigma_x$, σ_x should be approximately equal to $E\varepsilon_x$. This proves to be an excellent assumption. For example, for L = .0762m; W = 0.3048 m; E = 4.14e9Pa; Thickness, h = 23.4 microns; Average longitudinal tension, T_{avg} = 327N; R_w = 139m and θ_r = 0, the P. D. E. Model shows the error in the moment to be only 0.002 %. Even at R_w = 7m, the error is only 0.003 %.

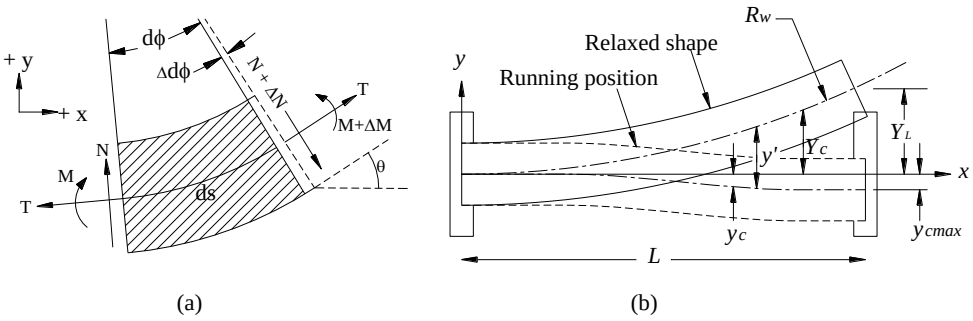

(a) (b)

Figure 9
Cambered web analysis
(a) Free body diagram (b) Solution parameters

The neutral axis offset, used in conventional curved bar theory and described in references such as Timoshenko [9], is important only for problems such as crane hooks that have large initial curvatures. For the curvatures experienced in web handling the offset is insignificant. Thus, development of the cambered model will begin with a uniform web model that will be transformed to the solution for a cambered web through a simple change of variable. One feature of curved bar theory that will be retained is the effect of longitudinal tension on curvature, introduced in equation (60). This adds a term to the solution that is important for a successful cambered web model.

In the following development y' will be used to indicate deflection of the uniform web under the influence of the cambered web boundary conditions and y_c will represent the sum of y' and the Y_c offset due to camber.

The free body diagram of Figure 9 (a) represents an infinitesimal segment of a uniform web under the influence of shear, longitudinal and bending stresses. The angle θ is assumed to be very small so that the forces N and $N + \Delta N$ are nearly parallel to the y-axis and $ds \cong dx$. Summing moments, taking clockwise as positive.

$$M - \left(M + \Delta M\right) + Ndx = 0 \qquad (53) \qquad \text{or} \qquad \frac{dM}{dx} = N \qquad (54)$$

Summing vertical forces taking $+y$ as positive.

$$N - \left(N + \Delta N\right) - Td\phi = 0 \qquad (55)$$

and since, $$d\phi \cong \frac{d^2y'}{d^2x}dx \qquad \frac{dN}{dx} = -T\frac{d^2y'}{dx^2} \ . \qquad (56)$$

Next, following Shelton's example [2], separate expressions for bending (subscript b) and shear (subscript s) will be developed.

$$\frac{dy'_s}{dx} = \frac{nN}{AG} \qquad (57)$$

where n is the correction factor for parabolic shear distribution, A is the cross sectional area and G is the shear modulus.

The action of the longitudinal force, T will increase angle $d\phi$ by,

$$\Delta d\phi = \frac{Tdx}{AEr} \qquad (58)$$

where r is the radius of curvature. And

$$\frac{1}{r} = \frac{d^2y'_b}{dx^2} \qquad (59)$$

So, taking into account the bending moment, M and the effect of (58) the total bending is,

$$\frac{d^2y'_b}{dx^2} = -\frac{M}{EI} + \frac{T}{AE}\frac{d^2y'_b}{dx^2} \qquad (60)$$

where I is the moment of inertia.

Conventional curved bar theory uses the initial curvature $1/r$ of the bar in the last term of (60) because the final curvature varies very little from the initial value. In this case, however, the bending is of the same magnitude as the initial curvature. So, the variable form of the curvature must be used. Now, since the total deflection is due to both bending and shear,

$$\frac{d^2y'_b}{dx^2} = \frac{d^2y'}{dx^2} - \frac{d^2y'_s}{dx^2} = \frac{d^2y'}{dx^2}\left(1 + \frac{nT}{AG}\right) \qquad (61)$$

Combining (61) and (60)

$$M = -EI\frac{d^2y'}{dx^2}\left(1 - \frac{T}{AE}\right)\left(1 + \frac{nT}{AG}\right) \ . \qquad (62)$$

Next, substituting (62) in (54) differentiating once and equating with (56)

$$\frac{d^4y'}{dx^4} - K_c{}^2\frac{d^2y'}{dx^2} = 0 \qquad (63)$$

where, $$K_c{}^2 = \frac{T}{EI\left(1 - \frac{T}{AE}\right)\left(1 + \frac{nT}{AG}\right)} \ . \qquad (64)$$

The only difference between this expression and the one in Shelton's dissertation [2] is an additional term in K_c to take better account of the effect of tension on curvature. For uniform webs the effect of *T/AE* is negligible. But, it is important for cambered webs.

Finally, to transform (63) into the cambered web equation a change of variable is made. Camber can be interpreted as an offset in the *y* coordinate of a uniform web.

$$y_c = Y_c + y' = \frac{x^2}{2R_w} + y' \tag{65}$$

where y_c is the *y* coordinate of the cambered web relative to $y = 0$ and the x^2 term approximates the arc of a circle with radius, R_w. Substituting this into (63) yields,

$$\frac{d^4 y'}{dx^4} - K_c{}^2 \frac{d^2 y'}{dx^2} = \frac{K_c}{R_w}. \tag{66}$$

Note that the dependent variable in this equation is still *y'* rather than y_c. So, when it is solved, equation (65) must be used again to yield the complete cambered web solution.

The solution of (66) is,

$$y' = -\frac{x^2}{2R_w} + C_1 \sinh(K_c x) + C_2 \cosh(K_c x) + C_3 x + C_4 \quad . \tag{67}$$

Substituting the result into (65) yields,

$$y_c = C_1 \sinh(K_c x) + C_2 \cosh(K_c x) + C_3 x + C_4 \tag{68}$$

Boundary conditions are:

$$@\, x = 0 :\ y_c = 0,\ \frac{dY_c}{dx} = \frac{nT_{avg}}{AG} \qquad @\, x = L :\ \frac{dy_c}{dx} = \theta_r,\ \frac{d^2 y_c}{dx^2} = \frac{1}{\rho_L} \tag{69}$$

where θ_r is the angle of the downstream roller, T_{avg} is the average longitudinal tension and ρ_L is the radius of curvature at the downstream roller. Note: the definition for the normal entry angle is θ_r instead of $\theta_r - \theta_c$ because of transformation (65). Using (65) in (62) the curvature at the downstream roller is,

$$\frac{1}{\rho_L} = \frac{1}{R_w} - \frac{M_L}{EI}\left(1 - \frac{T_{avg}}{AE}\right)^{-1}\left(1 + \frac{nT_{avg}}{AG}\right)^{-1} \tag{70}$$

The average longitudinal tension, T_{avg} is found from (43) as,

$$T_{avg} = Eh \int_{-W/2}^{W/2} \left[\frac{R_w - y_c}{R_w + W/2}\frac{V_u}{V_d}(1-\varepsilon_o)\right] dy_c = EWh\left[1 - \frac{V_u}{V_d}(1-\varepsilon_o)\left(1 + \frac{W}{2R_w}\right)^{-1}\right] \tag{71}$$

And M_L is found from (43) as

$$M_L = Eh \int_{-W/2}^{W/2} \left[\frac{R_w + W/2}{R_w - y_c}\frac{V_d}{V_u}(1+\varepsilon_o) - 1\right] y_c dy_c \,. \tag{72}$$

$$M_L = \frac{6EI}{W}\frac{V_d}{V_u}(1+\varepsilon_o)\left(1 + \frac{2R_w}{W}\right)\left[\frac{R_w}{W}\ln\left(\frac{-2R_w - W}{2R_w + W}\right) - 1\right] \tag{73}$$

So, the fourth boundary condition is,

$$\frac{1}{\rho_L} = \frac{1}{R_W}[\phi] \quad \text{where,} \quad \phi = 1 - \frac{V_u}{V_d}(1-\varepsilon_o)\left(1 + \frac{W}{2R_w}\right)^{-1}\left(1 - \frac{T_{avg}}{AE}\right)^{-1}\left(1 + \frac{nT_{avg}}{AG}\right)^{-1}. \tag{74}$$

Solving for C_1, C_2 and C_3,

$$C_1 = \left[-\frac{\theta_r}{K_c}\cosh\left(K_c L\right) + \frac{\phi}{R_w K_c^{\,2}}\sinh\left(K_c L\right) \right] \left[\cosh\left(K_c L\right)\left(1+\frac{nT_{avg}}{AG}\right) - 1 \right]^{-1}$$

$$C_2 = \left[\frac{\theta_r}{K_c}\sinh\left(K_c L\right) + \frac{\phi}{R_w K_c^{\,2}}\left(1+\frac{nT_{avg}}{AG} - \cosh\left(K_c L\right)\right) \right] \left[\cosh\left(K_c L\right)\left(1+\frac{nT_{avg}}{AG}\right) - 1 \right]^{-1}$$

$$C_3 = -C_1 K_c \left(1+\frac{nT_{avg}}{AG}\right)$$

$$C_4 = -C_2 \qquad (75)$$

Inspection of the coefficients reveals that each consists of two parts. One is proportional to the roller angle. The other (which will be called the camber term) is independent of the roller angle and proportional to end curvature, ϕ/R_w. Furthermore, the roller angle terms are exactly the same as for a uniform web. This makes sense; because as R_w approaches infinity, the camber terms should approach zero as the cambered web becomes more like a uniform web. So, to understand the general behavior of the cambered web solution it is only necessary to characterize the effect of the camber terms and add them to the misaligned roller results.

The change of variable made in equation (65) may be troubling to some. It looks like algebraic slight of hand. The thing to keep in mind is that it has been assumed that the slight curvature of the relaxed web has no effect on the size of the bending and shear deformations. Its main effect is to act as a *y* offset to the neutral axis of the beam. If the analysis had been carried without the variable change, it would have been possible to get the same result. But, the boundary conditions would have had to change in ways that might have been just as confusing. And it would have been necessary to add $x^2/(2Rw)$ to the result to account for the initial *y* offset. It could be rightfully argued that there must be some interaction between the initial curvature and the longitudinal tension. That is taken care of by the combined effects of new term that is introduced in equation (60) and the $1/R_w$ term in (70).

Normalizing the solution

A good way to normalize (68) is to divide y_c by the *y* displacement of the relaxed cambered web, $L/(2R_w)$, (Y_L in Figure 7). This quantity can then be graphed so that the combined effects of camber and roller misalignment can be estimated. Before doing that, however, it is necessary to point out some important relationships between the key variables. To do this a new parameter, β, is defined. It encompasses the main factors that determine longitudinal stress.

$$\beta = \frac{V_u}{V_d}\left(1-\varepsilon_o\right)\left(1+\frac{W}{2R_w}\right)^{-1} \qquad (76)$$

And a little algebra will show that,

$$\phi = 2n\frac{\left(\mu+1\right)\left(1-\beta\right)}{1+2n\left(1+\mu\right)\left(1-\beta\right)} \qquad (77) \quad \text{and} \quad \frac{nT_{avg}}{AG} = 2n\left(1+\mu\right)\left(1-\beta\right) \qquad (78)$$

and

$$K_c L = \frac{L}{W}\left\{\frac{12(1-\beta)}{\beta\left[1+2n(1+\mu)(1-\beta)\right]}\right\}^{.5} . \qquad (79)$$

Thus, it is possible to plot the camber portion of y_c as a function of only β and L/W (n and μ are treated as constants).

For parallel rollers, the ratio of longitudinal stress at the concave edge compared to the average stress will be approximately,

$$\frac{T_{edge\max}}{T_{avg}} = 1+\frac{\beta}{1-\beta}\left(1+\frac{W}{2R_w}\right) . \qquad (80)$$

The lateral force at the downstream end is,

$$N_L = -Eh\left(C_2\sinh(K_c L)+C_1\cosh(K_c L)\right)(1-\beta)\left(\frac{L}{W}\right)^{-1} K_c L . \qquad (81)$$

Comparison of the Beam and P. D. E. models

The solid lines in Figure 10 represent results from the beam model and the circles are data points from the P. D. E. model. Agreement between the two is excellent except for a slight deviation at L/W = 8 on the (1 - β) = 0.01 curve. In that case the P. D. E. model value is more likely right because it is more consistent with the curves below it. For values of (1 - β) > 0.01 both models should be used with caution because the magnitude of displacements, rotations or strains violate the assumptions of small deformation elasticity theory.

In conclusion, cambered webs do not cause large lateral misalignment. They do cause compressive stresses in the cross web direction that can cause wrinkling. And they can cause large cross web gradients in the longitudinal stress.

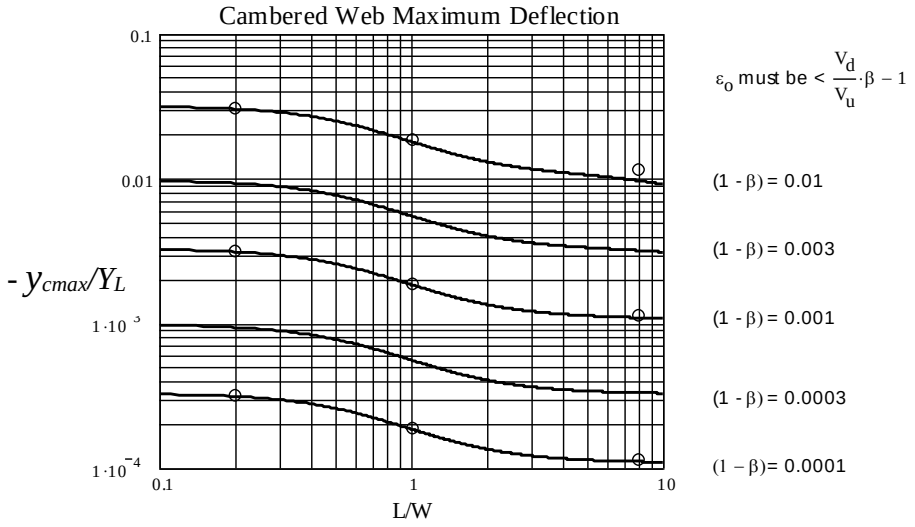

Figure 10
Comparison of Beam and P. D. E. Cambered Web Models
(Sign of the ordinate is reversed to facilitate logarithmic scaling.)

CONCLUSIONS

The scope of the individual studies in this paper was intentionally limited in favor of illustrating the range and versatility of the new method. But, it should be evident that:

- It has been shown that the new method can be successfully applied to the following situations.
  - The spreading behavior of concave and curved-axis rollers, including stress fields near the downstream roller.
  - The deflection and deformation of a cambered web.
  - The development of a beam theory model for a cambered web.
- The new method can evaluate the potential for damage to webs by producing precise and detailed descriptions of stress/strain fields throughout spans.
- It is evident that much more can be done in exploring these and other applications. Additional simplified models can be developed and where that is not possible results can be tabulated for everyday use.

Beyond illustrating the capabilities of the method, the following things have been accomplished.

- A beam model of the cambered web has been developed and shown to produce the same results as the new method for small strains.
- It has been shown that concave and curved-axis rollers behave very much alike and that concave rollers have an undeserved bad reputation.
- It has been shown that camber in a web can produce large variation in longitudinal stress across the width, but it does not cause large lateral alignment errors.

REFERENCES

1 Brown, J. L., "A New Method for Analyzing the Deformation and Lateral Translation of a Moving Web", Proceedings of the Eighth International Conference on Web Handling, June 2005

2 Shelton, J. J., "Lateral Dynamics of a Moving Web," Ph.D. Thesis, Oklahoma State University, Stillwater, Oklahoma, July 1968

3 Swanson, R. P., "Mechanics of Non-Uniform Webs," Proceedings of the Fifth International Conference on Web Handling, June 1999, pp 443 – 459

4 Swanson, R. P., "Testing and Analysis of Web Spreading and Anti-Wrinkle Devices," Proceedings of the Fourth International Conference on Web Handling, June 1997, pp 414 – 429

5 Shelton, J. J., "Effects of Web Camber on Web Handling," Proceedings of the Fourth International Conference on Web Handling, June 1997, pp 248 – 259

6 Markum, R. E., Good, J. K. “Design of Contoured Rollers for Web Spreading,” Proceedings of the Sixth International Conference on Web Handling, Oklahoma State University, June 2001, pp 567 – 582

7 Olsen, J. E., “Lateral Dynamics of an Imperfect Web,” Proceedings of the Sixth International Conference on Web Handling, Oklahoma State University, June 2001, pp 457 – 468

8 Novoshilov, V. V., “Foundations of the Nonlinear Theory of Elasticity”, Graylock Press, 1953

9 Timoshenko, S., “Strength of Materials”, Robert Kreiger Publishing Co., 1984